Intra-particle sorption rate and liquid chromatographic bandbroadening in porous polymer packings
III. Diffusion in the polymer matrix as the cause of slow sorption

Jingyi Li, Frederick F. Cantwell*

Department of Chemistry, University of Alberta, Edmonton, Alb., T6G 2G2, Canada

Abstract

In order to discover the physical cause of the slow intra-particle sorption rate of naphthalene in 10-μm spheres of the macroporous poly(styrene–divinylbenzene) (PS–DVB) polymeric HPLC sorbent Hamilton PRP-1, which has been shown to cause excessive bandbroadening of eluted peaks, the sorption-rate curve for naphthalene from methanol–water (85:15) was measured on PRP-1 using the shallow-bed technique. Sorption on PRP-1 follows a two-term theoretical rate equation for sorption on a biporous particle. From the (fast) first term it is found that 91% of the naphthalene is sorbed on the walls of the large pores and that the diffusion coefficient in these large pores is 3×10^{-6} cm^2/s. This is close to the free-solution diffusion coefficient, which demonstrates that large-pore diffusion is nearly unhindered. From the (slow) second term in the rate equation it is found that 9% of the naphthalene is sorbed into the polymer matrix of PRP-1, in which the effective diffusion coefficient is no larger than 10^{-12} cm^2/s. It is clear from these results that the cause of the slow intra-particle rate, and therefore of excessive chromatographic bandbroadening, is slow diffusion into the polymer matrix of PRP-1.

To provide additional information on the PS–DVB polymer matrix, the sorption rate of naphthalene was also measured on Hamilton PRP-∞ which is a 19-μm diameter, spherical, nominally nonporous PS–DVB chromatographic packing. The sorption is slow and follows the theoretical rate equation for hindered diffusion into a homogeneous sphere. The effective diffusion coefficient is $(4 \pm 1) \times 10^{-9}$ cm^2/s.

Diffusion through the polymer matrices in PRP-1 and PRP-∞ could be either hindered diffusion through micropores in a rigid matrix or diffusion through a flexible polymer 'gel'.

Keywords: Band broadening; Sorption; Stationary phases, LC; Polymer packings; Thermodynamic parameters; Kinetic studies

1. Introduction

In this laboratory, a shallow-bed heterogeneous kinetic technique was recently used to measure the intra-particle sorption-rate curve for the sorption of

naphthalene from methanol–water (85:15) onto the porous poly(styrene–divinylbenzene) (PS–DVB) HPLC packing Hamilton PRP-1 [1]. The measured rate, which was associated exclusively with processes taking place within the 10-μm diameter spheres of PRP-1, was combined with a recently elaborated mathematical model in order to predict

---

*Corresponding author

the characteristics that a chromatographic peak of naphthalene eluted from an HPLC column of PRP-1 would have if intra-particle rate processes constituted the only source of bandbroadening on the column [1,2]. The close agreement between the predicted elution peak and the experimentally observed elution peak demonstrated that, for naphthalene, intra-particle processes are, indeed, the major source of bandbroadening on PRP-1.

In the model employed to translate the sorption-rate curve into an elution peak, the former is curve-fit with a tri-exponential equation which, intentionally, is completely empirical and is not expressed in terms of physically significant parameters. Therefore, although the work unambiguously demonstrates that slow intra-particle rate processes are present in PRP-1, it does not identify the nature of those processes. That is the purpose of the presently reported work.

The general structural features of porous PS–DVB sorbents are well known [3–5]. The solid polymer matrix within the packing particle has the form of extensively fused, so-called 'microspheres'. The spaces between the fused microspheres is composed of macropores ($d_{pore} > 50$ nm) and mesopores ($2\ nm < d_{pore} < 50$ nm). The nominally non-porous polymer matrix may, in fact, be microporous. Micropores ($d_{pore} < 2$ nm) can be thought of as interstices between the polymer chains [6]. Pore-size distributions measured by nitrogen adsorption and size-exclusion chromatography typically show the presence of a substantial fraction of micropores in PS–DVB sorbents [7–10].

Often, the sorption of solutes by a macroporous PS–DVB sorbent is considered to involve only adsorption of the solute onto the surfaces of the polymer matrix which constitute the walls of the meso- and macropores (i.e., onto the outside of the fused microspheres) [11]. However, there is good evidence that solutes whose solubility parameters are similar to the solubility parameter of PS–DVB (i.e. $\delta \approx 9.1$ (cal/cm^3)$^{1/2}$) can diffuse into the polymer matrix [5,6,8,12,13]. Naphthalene, with a solubility parameter of 9.9 (cal/cm^3)$^{1/2}$ [14], is a solute that might be expected to do this. For diffusion through the matrix the diffusion coefficient would be unusually small. In contrast, diffusion through macro- and mesopores, whether it involves diffusion of dissolved solute through the stagnant mobile phase which fills the pores (i.e., pore diffusion) or diffusion of adsorbed solute along the pore walls (i.e., surface diffusion), will in either case be unhindered or only slightly hindered and therefore relatively fast and independent of the macro-/mesopore diameters [15–17].

If naphthalene is sorbed into the matrix as well as onto the meso-/macropore walls, the PRP-1 can be treated as a bidisperse (biporous) sorbent, for which the overall sorption rate can be described in terms of two effective diffusion coefficients, one for the meso-/macropores and one for the matrix [17–22]. In the presently reported study the shallow-bed sorption-rate curve for naphthalene on PRP-1 is evaluated in terms of a bidisperse diffusion model [21]. Also, the sorption rate of naphthalene is measured on a nominally nonporous PS–DVB sorbent, Hamilton PRP-∞, which, to a first approximation, represents the polymer matrix in PRP-1 [23]. In addition, the equilibrium amounts of naphthalene sorbed on PRP-1 and PRP-∞ are quantitatively compared. The present study clearly demonstrates that diffusion within the polymer matrix is the origin of the slow sorption of naphthalene on the macroporous polymer PRP-1 and, consequently, of the excessive bandbroadening and peak tailing seen in the elution peak for naphthalene on an HPLC column of PRP-1 [1].

2. Theory

The kinetic steps that are involved in the transfer of a solute molecule from the solution phase outside a macroporous sorbent particle to the sorbed state inside the particle have been described [2]. The shallow-bed technique which was used to measure the sorption rates creates infinite solution volume conditions and measures the combined rate effects of only those steps that take place within the particle. Furthermore, these rate measurements are made at naphthalene concentrations which are in the linear region of its sorption isotherm.

It is likely that the 'adsorption step', in which solute molecules transfer from the stagnant solution in the pores onto the polymer surface, is very fast

compared to the intra-particle diffusion steps, so that the adsorption step does not contribute to the measured sorption rate [17,24,25]. Therefore, it is likely that the rate determining process is 'particle mass-transfer' associated with intra-particle diffusion [26]. Two diffusion models are considered.

2.1. Monoporous diffusion model

If the sorbent particle can be treated as a homogeneous (monoporous, monodisperse) sphere, then diffusion can be described in terms of only one diffusion coefficient. In this context, a homogeneous particle could be either a particle in which only meso-/macropore diffusion occurs or a particle in which only matrix diffusion occurs. The sorption-rate curve measured under 'infinite solution volume' conditions would have the form:

$$F = \frac{n_t}{n_\infty} = 1 - \frac{6}{\pi^2} \sum_{m=1}^{\infty} \frac{1}{m^2} \exp(-\gamma \pi^2 m^2 t) \qquad (1)$$

where F is the fraction of the equilibrium amount of solute sorbed at time t; n_t and n_∞ are the moles of solute sorbed per gram of sorbent at time t and at equilibrium, respectively; m is an integer; and γ is defined as:

$$\gamma = \frac{D_{eff}}{r^2} \qquad (2)$$

where r is the radius of the spherical particle and D_{eff} is the 'effective diffusion coefficient' of the solute, which is a constant. Since sorption rates have been measured at concentrations that are in the linear region of the sorption isotherm, Eqs. 1 and 2 (and also 6 to 9, below) apply equally well to pore and surface diffusion [21,26–29]. However, detailed interpretation of D_{eff} differs for the two types of diffusion. It has been argued that with a liquid rather than a gas as the fluid filling the pores, pore diffusion is almost always dominant over surface diffusion [17]; although this view is not universally shared [27,30].

For macro-/mesopores diffusion in the solution phase will be assumed. The resulting equations (i.e., Eqs. 3 and 4) can be modified for surface diffusion, if that is desired [16,29]. The effective diffusion coefficient within the pores is related to the diffusion coefficient for free-diffusion in bulk solution, D_M, by the relationship [16,26,31,38]:

$$D_{eff} = \frac{D_M H_a}{(1 + R_a)\theta_a} \qquad (3)$$

in which H_a is a 'hindrance parameter' and θ_a is the tortuosity in the pore network. R_a is the equilibrium ratio of moles of solute sorbed on the pore walls to moles of solute dissolved in the solution in the pores, which is given by the expression:

$$R_a = \frac{\rho \kappa_a}{\epsilon_a} \qquad (4)$$

in which ρ is the density of the particle (g/cm^3), ϵ_a is the volume fraction of the particle that is due to the macro-/mesopores (i.e., particle porosity, ml/ml), and κ_a is the distribution coefficient of the solute, expressed as:

$$\kappa_a = \frac{(mol/g)_{adsorbed}}{(mol/ml)_{solution}} \qquad (5)$$

The quantity $(1 + R_a)^{-1}$ is the fraction of solute in the particle which is present in the pore solution and, therefore, free to diffuse. This is based on the usual assumption that within the pores, adsorption equilibrium is achieved instantaneously [28]. For diffusion in macropores the width of the pores is much greater than the size of the solute molecule so that the latter is diffusing unhindered through bulk liquid within these pores (i.e., $H_a = 1$). Diffusion in mesopores, which may be only several times wider than the solute molecule, may be slightly hindered.

Diffusion through the polymer matrix could involve either diffusion through micropores in a rigid polymer or diffusion through a flexible polymer 'gel'. In either case the effective diffusion coefficient $D_{i,eff}$ is much smaller than $D_{a,eff}$ in macro-/mesopores. If micropore diffusion is involved, then the 'hinderance parameter' $H_i < 1$ because the micropore is not much wider than the diffusing solute molecule [15,17,18,29,31–33]. In fact, for diffusion through narrow micropores the distinction between pore diffusion and surface diffusion is blurred. In contrast to H_i, the turtuosity factor θ is not strongly dependent on pore size and typically has a value between 2

and 6 for both macroporous and microporous materials [17,29,31–33].

If the polymer matrix is a gel, rather than being microporous, the solute may be thought of as dissolved in the very viscous polymer. Hence, in a gel $D_{i, \text{eff}}$ also would be very small.

2.2. Biporous diffusion model

The second diffusion model applies when the spherical particle is not homogeneous but, rather, is bidisperse. Both macro-/mesopore diffusion and matrix diffusion occur. If diffusion through the macro-/mesopores is considerably faster than diffusion through the matrix, then the sorption-rate equation is a relatively simple combination of two versions of Eq. 1, as follows [21]:

$$F = \frac{n_t}{n_\infty}$$

$$= \left[\left[1 - \frac{6}{\pi^2} \sum_{m=1}^{\infty} \frac{1}{m^2} \exp(-\gamma_a \pi^2 m^2 t) \right] \right.$$

$$+ \frac{\beta}{3\alpha} \left[1 - \frac{6}{\pi^2} \sum_{m=1}^{\infty} \frac{1}{m^2} \exp(-\alpha \gamma_a \pi^2 m^2 t) \right] \right]$$

$$\times \left[1 + \frac{\beta}{3\alpha} \right]^{-1} \tag{6}$$

where

$$\gamma_a = \frac{D_{a, \text{eff}}}{r_a^2} \tag{7}$$

$$\alpha = \frac{D_{i, \text{eff}} r_a^2}{D_{a, \text{eff}} r_i^2} \tag{8}$$

and

$$\beta = \frac{3(1 - \epsilon_a)\epsilon_i}{\epsilon_a} \frac{D_{i, \text{eff}}(1 + R_i) r_a^2}{D_{a, \text{eff}}(1 + R_a) r_i^2} \tag{9}$$

The subscript 'a' refers to the whole particle and to the macro-/mesopores, while the subscript 'i' refers to the matrix and to the microspherical aggregates within the particle.

The term $\beta/3\alpha$ in Eq. 6 is the ratio of the moles sorbed within the matrix to the moles sorbed in the

macro-/mesopores at equilibrium [21]. Non-linear curve fitting of Eq. 6 to sorption-rate data (n_t vs. t), as in Fig. 1, returns values for the constants γ_a, $\alpha\gamma_a$, $\beta/3\alpha$, and n_∞.

3. Experimental

3.1. Reagents and chemicals

Naphthalene, phloroglucinol, methanol, water, and methanol–water (85:15, v/v) were as previously described [1].

3.2. Sorbents

The macroporous PS–DVB sorbent PRP-1, 10±1 μm diameter spheres (Lot No. 334, Hamilton Co., Reno, NV, USA), was as previously described [1]. The nominally non-porous PS–DVB sorbent PRP-∞, 19±1 μm diameter spheres [34], was obtained as a gift from the same manufacturer (Hamilton).

3.3. Apparatus

The apparatus described in Ref. [1] was used in the shallow-bed mode to measure the sorption-rate curves of 4.9×10^{-6} mol/l of naphthalene on PRP-1 and 5.0×10^{-6} mol/l of naphthalene on PRP-∞, from 85% methanol.

The hold-up volume V_{HU} and the pore volume V_{PORE} for the 1.12×10^{-3} g bed of PRP-1 used in these studies were reported previously [1]. For the $(3.20 \pm 0.03) \times 10^{-3}$ g bed of PRP-∞, V_{HU} was 5.8 ± 0.5 μl and $V_{\text{PORE}} = 0$. The quantity V_{HU} was measured for the bed of PRP-∞ using a 7×10^{-5} mol/l solution of the unretained compound phloroglucinol in 85% methanol.

Calculation of moles of naphthalene sorbed per gram at a given time t, and at equilibrium, were performed using Eq. 1 in Ref. [1].

3.4. Shallow-bed conditions

The initial sorption rate of naphthalene on PRP-∞ was measured as a function of interstitial linear
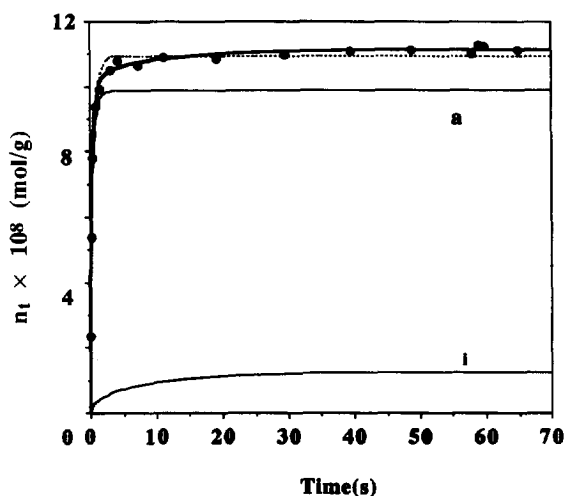
Fig. 1. Sorption-rate curve for naphthalene on PRP-1 from 85% methanol, compared to theory. Points are experimental from run 3 in Table 1. Light dashed line is fit by Eq. 1. Heavy solid line is fit by Eq. 6. Curves labeled 'a' and 'i' represent, respectively, the first (macro-/mesopore) term and the second (matrix) term in Eq. 6.

velocity of solution through the bed (U_{inter}) in order to identify the velocity above which sorption rate becomes independent of U_{inter}. At such velocities 'infinite bath' kinetic conditions are achieved and film diffusion is effectively eliminated as a contributor to the measured sorption rate. All subsequent measurements of sorption rate on PRP-∞ were performed at U_{inter} sufficiently high to meet these conditions. They were also performed in the linear region of the naphthalene sorption isotherm on PRP-∞.

4. Results and discussion

4.1. Sorption-rate curve on PRP-1

The data points in Fig. 1 for the sorption of naphthalene on the macroporous sorbent PRP-1 are for run 3 in Table 1. They are plotted here as moles sorbed per gram (n_t) versus time (t). The dashed line shows the fit of Eq. 1 to the data. This is for diffusion through a monoporous homogeneous sphere. It can be seen that Eq. 1 overestimates the rate between 2 and 10 s and underestimates the rate at times greater than about 30 s. Clearly, the slow sorption which occurs in the latter part of the sorption curve is not represented by Eq. 1.

The solid line through the data points in Fig. 1 shows the fit of Eq. 6, which is for diffusion through a biporous particle. This model gives a reasonable fit to the data at all times – short, intermediate and long. The two additional curves labeled 'a' and 'i' in Fig. 1 show the individual contributions of the two terms on the right-hand side of Eq. 6. These two curves are summed to give the solid fit line.

For the other three sorption-rate curves (runs 1, 2 and 4) that were also measured on the shallow bed of PRP-1 the results are similar; that is, Eq. 6 gives a reasonable fit while Eq. 1 underestimates rates at longer times. Shown in the first four rows of Table 1 are the values of the fitting parameters γ_a, $\alpha\gamma_a$, $\beta/3 \cdot \alpha$, and n_∞ which are obtained for each of the four kinetic runs on PRP-1. Average values are given in the fifth row.

From the parameter $\beta/3 \cdot \alpha$ it is readily calculated that $(9\pm3)\%$ of the total sorption capacity of PRP-1

Table 1
Fitting parameters of four rate curves for the sorption of naphthalene on PRP-1 from 85% methanol. Fit with Eq. 6

Run	γ_a (s^{-1})[a]	$\alpha\gamma_a$ (s^{-1})[b]	$\beta/3 \cdot \alpha$[c]	n_∞ (mol/g)
1	0.16	8.4×10^{-3}	0.077	1.04×10^{-7}
2	0.16	9.0×10^{-3}	0.060	1.14×10^{-7}
3	0.22	9.4×10^{-3}	0.127	1.11×10^{-7}
4	0.14	7.8×10^{-3}	0.117	0.86×10^{-7}
AVG	0.17 ± 0.03	$(8.6\pm0.7)\times10^{-3}$	0.10 ± 0.03	$(1.0\pm0.1)\times10^{-7}$

[a] $\gamma_a = D_{a,eff}/r_a^2$; $r_a = 5$ μm.
[b] $\alpha\gamma_a = D_{i,eff}/r_i^2$.
[c] $\beta/3 \cdot \alpha$=(mol in micropores/mol in macro- and mesopores).

for naphthalene is due to sorption within the matrix and the remaining $(91\pm3)\%$ is due to surface adsorption on the walls of the macro-/mesopores.

4.2. Diffusion in large pores of PRP-1

The effective diffusion coefficient of naphthalene in the meso- and macropores is $D_{a, \text{eff}} = (4.2\pm0.8) \times 10^{-8}$ cm^2/s. It is obtained by multiplying γ_a by $(5.0\times10^{-4}$ cm$)^2$, the square of the radius of a PRP-1 particle. The product of the diffusion coefficient and the hinderance parameter, $D_M H_a$, may be obtained by substituting $\theta_a = 3\pm1$ [32] and $R_a = 24\pm3$ into Eq. 3. This value of R_a is calculated from Eq. 4 in which $\rho = 0.61$ g/ml, $\epsilon_a = 0.48$ ml pore/ml particle [1,35] and κ_a is:

$$\kappa_a = \frac{0.91 n_\infty}{C_M} = 19\pm2 \text{ ml/g} \tag{10}$$

In Eq. 10, $n_\infty = 1.0 \times 10^{-7}$ mol/g from Table 1, $C_M = 4.90 \times 10^{-9}$ mol/ml and 0.91 is the mean fraction of naphthalene adsorbed in the macro-/mesopores, as determined above.

The product $D_M H_a$, calculated in this way, is $(0.3\pm0.1)\times10^{-5}$ cm^2/s. The expected value of D_M for free-solution diffusion of naphthalene in methanol–water (85:15) can be estimated to be $D_M = (1.1\pm0.2) \times 10^{-5}$ cm^2/s via the Wilke–Chang equation [36]. In calculating the latter value both the solvent association parameter and the solvent molecular mass for methanol–water (85:15) were taken to be the volume-fraction-based arithmetic mean values of the pure solvents methanol and water; and the molar volume of naphthalene was taken to be 112 cm^3/mol [37].

Comparison of the Wilke–Chang value of D_M with the value of $D_M H_a$ gives $H_a = 0.27\pm0.09$ which represents only very slight hinderance. Its significance can be seen as follows. Hindered diffusion has been the subject of numerous studies [14,32,38–41]. The hindrance parameter is the ratio of the diffusion coefficient in the pores to that in free solution. Hindrance can be thought to result both from increasing frictional drag and from steric exclusion of solute from an increasing fraction of the pore cross section, as the ratio of solute diameter (e.g., d_{naph}) to pore diameter (i.e., d_{pore}) increases toward a value of

1. For $(d_{\text{naph}}/d_{\text{pore}}) \lesssim 0.9$, H is given by the expression:

$$H = \frac{\left(1 - \dfrac{d_{\text{naph}}}{d_{\text{pore}}}\right)^2}{K_1} \tag{11}$$

where K_1 is a complex function of $d_{\text{naph}}/d_{\text{pore}}$, for which values have been tabulated [38].

The value $H_a = 0.27\pm0.09$ which is found in the present case, corresponds to the ratio $d_{\text{naph}}/d_{\text{pore}} = 0.26\pm0.06$. Since the diameter of a naphthalene molecule is about 6.2 Å, the above value of H_a implies that the observed rate of pore diffusion in the larger pores in PRP-1 is governed by mesopores with diameters in the range of 24 Å. This seems quite reasonable in light of the reported average meso-/macropore diameter of 75 Å [35].

4.3. Diffusion in polymer matrix of PRP-1

From the curve-fitting parameter $\alpha\gamma_a$, the ratio $D_{i,\text{eff}}/r_i^2$ is found to be $(8.6\pm0.7)\times10^{-3}$ s^{-1}. Unlike the situation for large-pore diffusion in which r_a is known, the radius r_i for the fused 'microspherical aggregates' within the particle is not known. Electron micrographs of related macroporous PS–DVB polymers, having larger macropores than PRP-1, show microspherical aggregates having about 0.3 μm diameter [9]. If the situation is about the same in PRP-1, then the radius r_i of a microspherical aggregate would be roughly 0.1 μm. From Eq. 2, this would correspond to $D_{i, \text{eff}} \approx 10^{-12}$ cm^2/s.

The question of whether the matrix can be treated as a rigid polymer containing micropores through which naphthalene diffusion via pore- or surface diffusion or whether it should be treated as a flexible polymer gel through which naphthalene diffuses, cannot be answered in the present study. It may be noted that if micropore diffusion is involved the diameter of the micropores would have to be quite close to the diameter of the naphthalene molecule [38–41].

4.4. Diffusion in polymer matrix of PRP-∞

In order to provide additional support for the view that naphthalene diffuses into the polymer matrix of

PRP-1, the sorption rate of naphthalene was measured on the nominally nonporous sorbent PRP-∞ using the shallow-bed technique. The particles are spherical with a diameter of 19 ± 1 μm. Shown in Fig. 2 is a sorption-rate curve (run 1) for naphthalene on PRP-∞ from 85% methanol. The points are experimental and the solid line shows the non-linear least squares fit of the data by Eq. 1, for diffusion through a homogeneous sphere. Presented in Table 2 are the fitting parameters γ and n_∞ that are obtained for both run 1 and run 2 on PRP-∞. The effective diffusion coefficient for naphthalene in PRP-∞, $D_{eff} = (4 \pm 1) \times 10^{-9}$ cm^2/s, is obtained by multiplying γ by r^2.

Naphthalene diffuses into the polymer matrix of the nominally nonporous particles of PRP-∞ and this diffusion is characterized by a single diffusion coefficient. The analogy with the second term of Eq. 6, as applied to PRP-1, is clear and the results support the view that naphthalene diffuses into the polymer matrix of PRP-1. However, the effective diffusion coefficient on PRP-∞ is several orders of magnitude greater than that for the matrix of PRP-1. This difference is not surprising. Whether hindered micropore diffusion or gel diffusion is occurring in these two matrices, the diffusion coefficient would be a strong function of the matrix structure. Perhaps there is a small difference in the average degree of
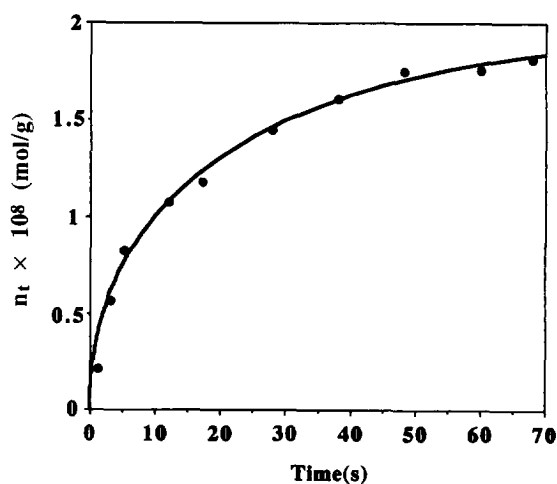
Table 2
Fitting parameters of two rate curves for the sorption of naphthalene on a 3.2-mg bed of PRP-∞ from 85% methanol. Fit with Eq. 1

Run	γ (s^{-1})[a]	n_∞ (mol/g)
1	3.2×10^{-3}	2.0×10^{-8}
2	5.3×10^{-3}	2.0×10^{-8}

[a] $\gamma = D_{eff}/r^2$; $r = 9.5 \pm 0.5$ μm.

polymerization between the PRP-1 and PRP-∞ matrices or perhaps the polymerization rate is slower during the synthesis of PRP-1, so that the resulting polymer matrix is more homogeneous or the polymer chains have somewhat less flexibility [6].

4.5. Equilibrium sorption

The data reported in Table 1 for PRP-1 and in Table 2 for PRP-∞ were obtained at essentially the same solution concentration of naphthalene in 85% methanol, which is well within the linear regions of the sorption isotherms for naphthalene [1]. Therefore it is possible to compare the equilibrium concentrations of sorbed naphthalene (i.e., n_∞, mol/g) on PRP-1 and PRP-∞. The equilibrium concentration on PRP-∞ is 2.0×10^{-8} mol/g. On PRP-1, the total equilibrium concentration is 1.0×10^{-7} mol/g, but only $(9 \pm 3)\%$, or 0.9×10^{-8} mol/g, of the equilibrium amount follows the slow, second term in Eq. 6. The equilibrium concentration of 0.9×10^{-8} mol/g is in very reasonable agreement with the concentration of 2.0×10^{-8} mol/g sorbed on PRP-∞. This demonstrates that the chemical character of the matrices in these two polymers are similar and is consistent with the conclusion from the kinetic argument that slow sorption on PRP-1 is, in fact, diffusion through the polymer matrix.

Acknowledgments

Fig. 2. Sorption-rate curve for naphthalene on PRP-∞ from 85% methanol, compared to theory. Points are experimental. Line is fit by Eq. 1.

References

[1] J.Y. Li, L. Litwinson and F.F. Cantwell, J. Chromatogr. A, 726 (1996) 25.

[2] D. Gowanlock and F.F. Cantwell, J. Chromatogr. A, 726 (1996) 1.

[3] R.L. Albright, Reactive Polymers, 4 (1986) 155.

[4] K. Kun and R. Kunin, J. Polym. Sci. Part A1, 6 (1968) 2689.

[5] P. Cornel and H. Sontheimer, Chem. Eng. Sci., 41 (1986) 1791.

[6] F. Nevejans and M. Verzele, J. Chromatogr., 406 (1987) 325.

[7] F. Nevejans and M. Verzele, Chromatographia, 20 (1985) 173.

[8] N. Tanaka, T. Ebata, K. Hashizume, K. Hosoya and M. Araki, J. Chromatogr., 475 (1989) 195.

[9] H. Jacobelli, M. Bartholin and A. Guyot, J. Appl. Polym. Sci., 23 (1979) 927.

[10] K. Jarabek, Anal. Chem., 57 (1985) 1598.

[11] D.J. Pietrzyk, in P.R. Brown and R.A. Hartwick (Editors), High Performance Liquid Chromatography (Chem. Anal.), Vol. 98, Wiley, New York, 1989, Chapter 10.

[12] P. Cornel, H. Sontheimer, R.S. Summers and P.V. Roberts, Chem. Eng. Sci., 41 (1986) 1801.

[13] D. Liru, H. Xizhang, W. Quhui, M. Qingcheng, L. Yuliang and Z. Youliang, Scientia Sinica (Series B), 25 (1982) 905.

[14] Handbook of Chemistry and Physics, CRC Press, Boca Raton, FL, 70th ed., 1989, p. C-681.

[15] M. Suzuki, Adsorption Engineering, Elsevier, Amsterdam, 1990, Chapters 4–7.

[16] D.M. Ruthven, Principles of Adsorption and Adsorption Processes, Wiley, New York, 1984, Chapters 5 and 6.

[17] D.M. Ruthven, in A.E. Rodrigues, M.D. LeVan and D. Tondeur (Editors), Adsorption Sci. Technol.: NATO Adv. Study Inst. on Adsorption: Sci. Technol. Proceedings, Vol. 158, Kluwer Academic Pub., Boston, 1988, pp. 87–114.

[18] R.G. Peel and A. Benedek, J. Environ. Eng. Div. Am. Civil Eng., 106 (EE4) (1980) 797.

[19] R.G. Peel and A. Benedek, Environ. Sci. Technol., 14 (1980) 66.

[20] R.G. Peel and A. Benedek and C.M. Crow, Am. Inst. Chem. Eng., 27 (1981) 26.

[21] E. Ruckenstein, A.S. Vadyanathan and G.R. Youngquist, Chem. Eng. Sci., 26 (1971) 1305.

[22] W.J. Weber and S. Liang, Environ. Prog., 2 (1983) 167.

[23] D.P. Lee, J. Chromatogr., 443 (1988) 143.

[24] J.C. Giddings, Dynamics of Chromatography, Dekker, New York, 1965, Chapters 2 and 6.

[25] J.M. Smith, in W.J. Weber, Jr. and E. Matijevic (Editors), Adsorption from Aqueous Solution: ACS Symp. Ser., Vol. 79, American Chemical Society, Washington, DC, 1968, pp. 8–22.

[26] F. Helfferich, Ion Exchange, McGraw-Hill, New York, 1962, Chapters 6 and 9.

[27] A.A. Aguwa, J.W. Patterson, C.N. Haas and K.E. Noll, J. Water Pollut. Control Fed., 56 (1984) 442.

[28] J. Crank, The Mathematics of Diffusion, Oxford University Press, London, 1975, Chapters 6 and 14.

[29] M.L. Brusseau and P.S.C. Rao, CRC Crit. Rev. in Environmental Contamination, 19 (1989) 33.

[30] D.W. Hand, J.C. Crittenden and W.E. Thacker, J. Env. Eng. Div. Am. Soc. Civil Engrs., 109 (1983) 82.

[31] D.D. Frey, E. Schweinheim and C. Horvath, Biotechnol. Prog., 9 (1993) 273.

[32] C.K. Colton, C.N. Satterfield and C.J. Lai, J. Am. Inst. Chem. Eng., 21 (1975) 289.

[33] J.C. Giddings, Dynamics of Chromatography, Dekker, New York, NY, 1965, Chapter 6.

[34] Private communication, Hamilton Co., Reno, NV.

[35] Technical Information Sheet for PRP-1, Hamilton Co., Reno, NV.

[36] C.R. Wilke and P. Chang, J. Am. Inst. Chem. Eng., 1 (1955) 264.

[37] J.T. Edwards, J. Chem. Ed., 47 (1970) 261.

[38] P.L. Paine and P. Scherr, Biophys. J., 15 (1975) 1087.

[39] W.M. Deen, J. Am. Inst. Chem. Eng., 33 (1987) 1409.

[40] G.M. Mavrovouniotis and H. Brenner, J. Colloid Interface Sci., 124 (1988) 269.

[41] H. Brenner and L. Gaydos, J. Colloid Interface Sci., 58 (1977) 312.